

Size Exclusion Chromatography with Viscosity Detection of Complex Polysaccharides: Component Analysis

Peter D. Hoagland,*† Marshall L. Fishman,† Gordana Konja,‡ and Ekkehard Claus†

Eastern Regional Research Center, Agricultural Research Service, U.S. Department of Agriculture, 600 East Mermaid Lane, Philadelphia, Pennsylvania 19118, and Faculty of Food and Biotechnology, University of Zagreb, Zagreb, Croatia

Complex polysaccharides obtained from plants and microbes are finding increased application in the food industry as additives to improve the functional properties of processed foods. High-performance size exclusion chromatography (HPSEC) with concentration-viscosity detection, coupled with Gaussian curve fitting of concentration and viscosity chromatograms, a method earlier developed to investigate the behavior of a variety of pectins in solution, has now been applied to tragacanthin, gum locust bean, (carboxymethyl)cellulose, sodium alginates, apple pectin, and gum arabic. Weight-average intrinsic viscosities (i.v.) were determined directly from areas under the concentration and specific viscosity curves. In addition, global and component radii of gyration (R_{gw}) and molecular weights (MW_w) were determined from both size and universal calibration of columns with pullulans. Gaussian component i.v. and component R_{gw} values of some polysaccharides, investigated in 0.05 M NaNO₃ at 35 °C, were found to be related by a characteristic power law exponent. HPSEC with concentration and viscosity detection has good potential for rapidly determining physical properties crucial to control of quality of polysaccharides in the food industry.

INTRODUCTION

Recent studies of pectin by high-performance size exclusion chromatography (HPSEC) using both concentration and viscosity detection have suggested that pectin chromatograms can be analyzed in terms of a few Gaussian components (Fishman et al., 1989b, 1991a,b). Global values for radius of gyration (R_g), intrinsic viscosity (i.v.), and molecular weight (MW) can be calculated from component properties determined by universal calibration (Fishman et al., 1991a). We have extended this analysis to some polysaccharide gums of interest to the food industry with the goal of applying HPSEC with concentration-viscosity detection to uniquely characterize these biopolymers in small volumes of dilute aqueous solution. In addition, such analysis could be a powerful tool in following subtle and major changes in polysaccharide size and viscosity that are caused by heating, microwaving, aging, chemical modification, enzymatic degradation, or adulteration.

EXPERIMENTAL PROCEDURES

Materials. Gum locust bean and gum tragacanth were purchased from U.S. Biochemical. Gum arabic and sodium alginates IV, VI, and VII were products of Sigma Chemical Co. Water-soluble fractions of these gums were prepared by gentle stirring of 1% mixtures at room temperature for 1 h. The solutions were filtered through 0.45- μ m pore diameter Nucleopore membrane filters before injection. The water-soluble fraction of gum tragacanth is referred to as tragacanthin.

Size Exclusion Chromatography. Waters μ -Bondagel E-High, E-1000, and SynChrom Synchronapak GPC-100 columns were used in series and maintained at 35 \pm 0.1 °C in a thermoregulated water bath. The mobile phase was 0.05 M NaNO₃ prepared with house-distilled water treated with a Modulab polisher (Continental Water Systems Corp.) and filtered with a 0.2- μ m Nucleopore membrane before degassing. A front-end Degasser ERC-3120 (Erma Optical Works, Ltd.) was connected to a Beckman

Model 110 pump with a Model 421 controller. The pump output was fed to a Beckman pulse filter and two Waters M45 pulse dampeners. Samples were introduced with a Beckman Model 210 injector valve fitted with a 100- μ L sample loop. Nominal flow rate was 0.5 mL/min. Actual flow rate was measured with a 2-mL pipet horizontally connected to the RI detector outlet. A ca. 0.1-mL bubble was injected into the exit stream, and its passage through a known volume in the pipet was accurately timed with a stopwatch (Fishman et al., 1987). Flow rates were also calculated from the maximum peak position for material eluting at the total volume (V_t) of the system. This volume was found to be 8.20 mL from sucrose chromatograms. Observed short-term flow rate variation was <0.5%. Concentration was measured by differential refractive index with a RI detector Model 7510 (Erma Optical Works) with 30 \times preamplification of its 0-1-V integrator output. The detector was calibrated with dextran standards and up to 8 mg/mL gave a linear response (correlation coefficient 0.999) with slope of 4843 \pm 68 mV mg⁻¹ mL⁻¹ (in the RI detector cell). The observed RI (differential refractive index) was never above 500 mV, so that the concentration at which the viscosity was determined was always less than 0.1 mg/mL (0.01%). A differential viscometer Model 100 (Viscotek Corp.) was operated at 35 °C with periodic re-zeroing of the inlet pressure at zero flow to correct for drift we observed to be related to overnight variation in room temperature. The specific viscosity, η_{sp} , is defined by the relationship (eq 1) between excess pressure (DP, mV) of the polymer solution over that of the solvent (mobile phase) and the inlet pressure (P_0 , mV), which is the pressure due to the mobile phase.

$$\eta_{sp} = \frac{4 \times DP}{P_0 - (2 \times DP)} \quad (1)$$

In dilute solution, we assumed that i.v. $\approx \eta_{sp}/c$, where c is the concentration of solute. Furthermore, for pectins Fishman et al. (1989a) found that the area under the excess pressure (DP) response curve gives the observed i.v. for the whole injected sample. We checked the above assumption with pullulan standards P-10, P-20, P-50, P-100, P-200, P-400, and P-800 from Polymer Laboratories. A plot of the measured i.v. against literature i.v. for pullulans produced a straight line that passed through zero (Figure 1). The integrator output of each detector was converted with a DT5712-PGL (Data Translation) A/D board installed in an IBM compatible PC. The digitized signals were processed with Unical 3.11 software from Viscotek. The Asyst

* Author to whom correspondence should be addressed.

† U.S. Department of Agriculture.

‡ University of Zagreb.

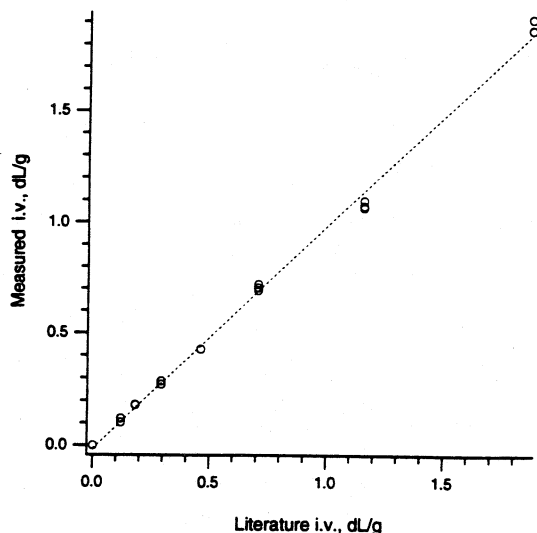


Figure 1. 1. Measured i.v. for pullulan standards (P-10, P-20, P-50, P-100, P-200, P-400, and P-800) compared to literature values in Table I (Fishman et al., 1987): slope = 1.00 ± 0.01 with a correlation coefficient of 0.998.

Table I. Weight-Average Radius of Gyration (R_{gw}) Values for Pullulan Standards Obtained from Equations in Figure 2

pullulan standard	M_w^a	[i.v.], ^a dL/g	polydispersity, ^a M_w/M_n	R_{gs} , nm	R_{gw} , nm
P-10	12 200	0.119	1.05	3.51	3.42
P-20	23 700	0.181	1.01	4.95	4.93
P-50	48 000	0.286	1.02	7.33	7.25
P-100	100 000	0.459	1.05	11.1	10.8
P-200	186 000	0.704	1.11	16.1	15.2
P-400	380 000	1.155	1.05	23.1	22.5
P-800	853 000	1.865	1.00	35.1	35.1

^a Polymer Laboratories. ^b $R_{gw} = R_{gs}[(M_w/M_n)^{1/1.8}]$.

*.DAT files acquired with the Unical program were converted to ASCII text files for use by other programs. For the highest viscosity pullulan (P-800) the observed DP (excess pressure) response/RI (refractive index) response was flat with elution volume. This observation was further evidence that the concentration of polysaccharide in the pressure transducer cell was low enough for the approximation $i.v. \approx \eta_{sp}/c$ to be valid.

Column Calibration. The column set was calibrated with the seven narrow distribution pullulan standards above. The supplier furnished weight-average molecular weights (M_w) from light scattering, polydispersities (M_w/M_n) from equilibrium sedimentation, and i.v. values (Fishman et al., 1987). Weight-average radius of gyration (R_{gw}) values for these pullulans were obtained by curve fitting published values for pullulan M_w , R_{gs} (nanometers), and i.v. (deciliters per gram) (Kato et al., 1982) to eqs 2 and 3, the Stokes-Einstein equation (Flory, 1953).

$$MW_w = A(R_{gw})^d \quad (2)$$

$$MW_w(i.v.) = B(R_{gw})^{3.000} \quad (3)$$

$$A = 1291 \quad B = 35.76 \quad d = 1.825$$

R_{gw} values are listed in Table I, and the fitted power law curves are shown in Figure 2. The elution volume, V_e , for each pullulan standard was determined by the peak maximum of the Gaussian curve that fitted its concentration (RI) response curve. The sigma (half-width at half-height) for each Gaussian curve was found to vary with elution volume and, therefore, hydrodynamic volume and was employed as an empirical measure of the band spreading for each pullulan (see below). Void volumes (V_0) and total volumes (V_t) were measured with established methods (Fishman et al., 1987) and were used to calculate the distribution coefficient, K_{AV} , from V_e with

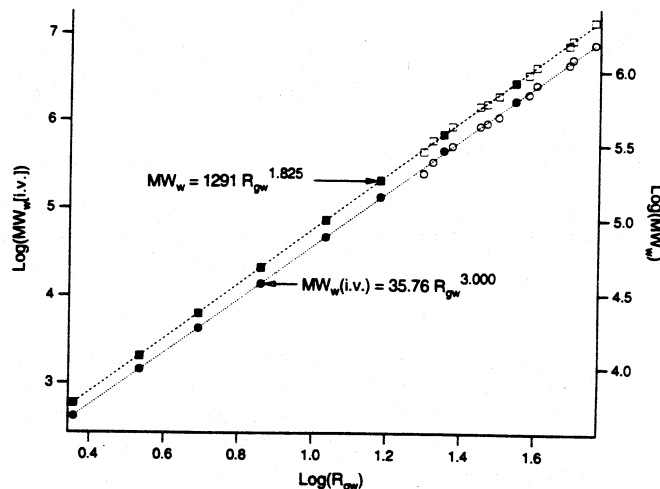


Figure 2. Fitted curves used to determine R_{gw} values for pullulan standards in Table I. Solid circles and squares are pullulan values in Table I and P-5. Open circles and squares are pullulan values from Kato et al. (1982).

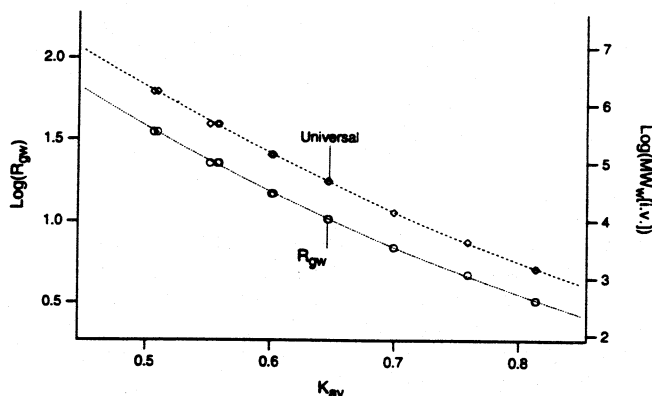


Figure 3. Size (R_{gw}) and universal (MW_w [i.v.]) calibration curves for column set based on distribution coefficients (K_{AV}) for pullulan standards.

$$K_{AV} = (V_e - V_0)/(V_t - V_0) \quad (4)$$

Calibration curves for $\log(R_{gw})$ and $\log(MW_w$ [i.v.]), a universal plot, were constructed as before (Fishman et al., 1987) and are reproduced in Figure 3.

Component Analysis. We have refined a method to extract information from HPSE chromatograms by fitting a series of Gaussian components to a set of concentration and viscosity response curves. A Gaussian component is characterized by its peak elution volume, peak height, and sigma. The number of Gaussian components required to fit a given response curve is determined by the total volume required to elute the polysaccharide and the sigmas assigned to the Gaussian components. In practice, peak elution volumes of neighboring Gaussian components differ by roughly the sum of their sigmas. In earlier studies (Fishman et al., 1991b), only two values for sigma were applied to curve fitting. They were 0.274 mL for large R_g components and 0.11 mL for small R_g components. As noted above, we have now observed that response curves for pullulan standards can be fitted by one Gaussian curve and that the sigma derived therefrom exhibits a distinct dependence on peak elution volume. In Figure 4 is shown the power plot for Gaussian sigma and pullulan K_{AV} . The linear best fit allows the sigma of each Gaussian component to be related to the component elution volume during curve fitting. Furthermore, up to now, a concentration response curve was first fitted by a set of Gaussian components. The component elution volumes were then fixed and the same component peak positions were applied to fitting the excess pressure response curve after adjustment for detector offset. In this case, only the viscosity component heights were allowed to vary to obtain a fit. We have revised this approach by appending to the RI response curve the excess pressure

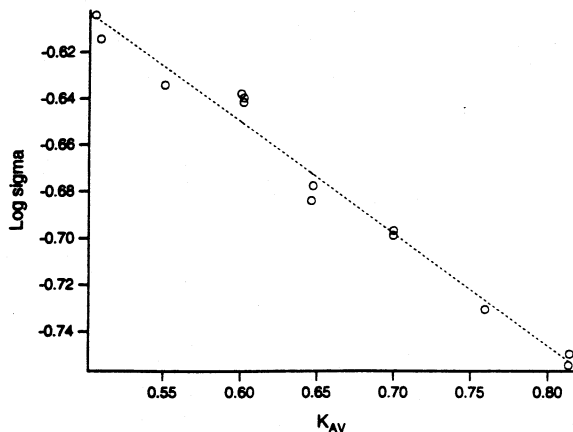


Figure 4. Sigmas for Gaussian curve fitted to pullulan RI response curves plotted as a function of K_{AV} . Linear fit was used for eq 9.

response suitably displaced by 4–5 mL to avoid signal overlap. This provides one array of data points which could be fitted by standard nonlinear procedures. The Macintosh graphics program, Igor v1.24 (WaveMetrics, Lake Oswego, OR), features user-defined curve fitting functions with up to 20 variables. The program implements standard Gauss-Newton procedures for nonlinear curve fitting (Press et al., 1988). We adapted this program to use up to 13 Gaussian components to fit the combined concentration and viscosity response curve with eq 5. The elution time of a given viscosity Gaussian component was set equal to the time for the corresponding concentration component plus its displacement corrected for detector offset (eq 7). Thus, up to

$$\text{fitted response area} = \sum_{i=8}^{17} \left[\sum_{i=1}^7 RI_{it} + \sum_{j=1}^6 DP_{j(t+\text{displace})} \right] \quad (5)$$

$$RI_{it} = \sum_{i=8}^{17} (h_{RI_i}) \exp \left[- \left[\frac{(T_{RI_i} - t)^2}{2\sigma_i^2} \right] \right] \quad (6)$$

7 variables representing elution times of concentration components and up to 13 or 14 variables representing heights of both concentration and viscosity components were used to fit a combined response curve (eq 6). Initial estimates for variables were made to approximate a fit. In all cases the fitting procedure was well-behaved since the variables were constrained by two independent regions of the combined response curve.

$$DP_{j(t+\text{displace})} = \sum_{i=8}^{17} (h_{P_j}) \exp \left[- \left[\frac{(T_{RI_i} + \text{displace} - t)^2}{2\sigma_i^2} \right] \right] \quad (7)$$

$$\text{displace (min)} = (5 - 0.1074)(\text{mL}) / [\text{FR}(\text{min/mL})] \quad (8)$$

For the combined response (eq 5) at time t , RI_{it} is the RI response for each component i and $DP_{j(t+\text{displace})}$ is the excess pressure response for corresponding component j . The smallest concentration component ($i = 7$) usually did not have detectable viscosity. T_{RI_i} and h_{RI_i} were concentration component i elution time and height at peak maximum, respectively, and h_{P_j} was viscosity component j peak height. FR was the flow rate. Component sigma (σ_i) was related to T_{RI_i} (component i elution time) through eq 9 obtained from the linear best fit of the plot in Figure 4 with the following assumptions:

$$\text{maximum } \sigma = 0.26 \text{ mL} \quad \text{minimum } \sigma = 0.12 \text{ mL}$$

$$\log(\sigma) = -0.602 - 0.106 T_{RI_i} \times \text{FR} - \log(\text{FR}) \quad (9)$$

Global weight average i.v. was calculated as the sum of the products of component weight fraction and component i.v. A fitted i.v. response curve was calculated for each point of the

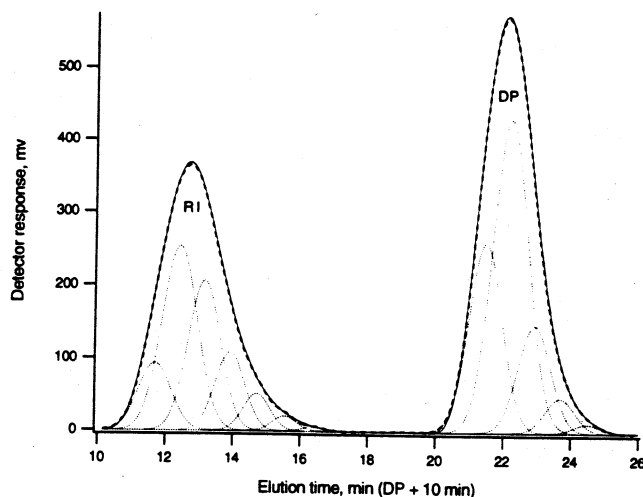


Figure 5. Twelve Gaussian curves fitted to combined concentration (RI) and viscosity (excess pressure, DP) response curve for alginate VI. Components are numbered from left to right in decreasing size.

fitted concentration response curve with

$$IV_{\text{fitted}} = \frac{\sum_{i=1}^6 IV_i \times (h_{RI_i}) \exp \left[- \left[\frac{(T_{RI_i} - t)^2}{2\sigma_i^2} \right] \right]}{\sum_{i=1}^6 (h_{RI_i}) \exp \left[- \left[\frac{(T_{RI_i} - t)^2}{2\sigma_i^2} \right] \right]} \quad (10)$$

This curve was then compared to its corresponding fitted R_{gw} response curve calculated similarly with

$$R_{g \text{ fitted}} = \frac{\sum_{i=1}^7 R_{g_i} \times (h_{RI_i}) \exp \left[- \left[\frac{(T_{RI_i} - t)^2}{2\sigma_i^2} \right] \right]}{\sum_{i=1}^7 (h_{RI_i}) \exp \left[- \left[\frac{(T_{RI_i} - t)^2}{2\sigma_i^2} \right] \right]} \quad (11)$$

RESULTS AND DISCUSSION

Component Analysis. A representative fitted combined response curve is shown in Figure 5. The salient feature of this approach is that both concentration and viscosity response data contribute to determination of fitted elution volume, and thereby R_{gw} , for the large components (usually 1, 2, and 3). Values for component R_{gw} , weight fraction, i.v., and MW_w are listed in Table II. The estimate of precision for component analysis was based on 14 runs. With the exception of apple pectin, which has low viscosity, component 1 error for R_{gw} was <2% and for i.v. was <3%; component 2 error for R_{gw} was <4% and for i.v. was <6%. Other components had errors for R_{gw} of <6%. Components with low i.v. and low weight fraction had larger errors due to low signal-to-noise ratios. The component errors for apple pectin were about 2.5-fold greater than the above values. The precision for component analysis can be excellent under closely controlled column and room temperature, pulse dampening, flow rate, and sample preparation. The accuracy for component analysis is ultimately determined by column calibration and needs to be evaluated with a series of well-characterized broad R_{gw} , i.v., and MW_w distribution polysaccharides.

Tragacanthin. The HPSE chromatogram was fitted by seven concentration components and five viscosity components (Figure 6). A global MW_w of 502 000, global

Table II. Properties of Components

	component							wt av
	1	2	3	4	5	6	7	
tragacanthin								
R_g , nm	85.0	42.9	20.3	11.1	7.1	4.7	3.3	43
wt fraction	0.273	0.321	0.187	0.102	0.076	0.032	0.012	
$[\eta]$, dL/g	17.6	5.9	2.1	1.2	a	a	a	7.2
MW, ($\times 10^{-3}$)	1147	490	150	47	a	a	a	502
gum locust bean								
R_g , nm	60.3	36.1	20.6	12.0	7.2	4.3	a	43
wt fraction	0.446	0.337	0.135	0.051	0.022	0.011	a	
$[\eta]$, dL/g	12.3	10.4	6.8	6.2	a	a	a	10.2
MW, ($\times 10^{-3}$)	622	168	48	10	a	a	a	341
(carboxymethyl)cellulose								
R_g , nm	71.9	39.9	21.9	13.0	8.6	6.1	4.2	33
wt fraction	0.157	0.335	0.247	0.132	0.076	0.035	0.017	
$[\eta]$, dL/g	21.0	12.3	6.9	4.0	2.2	a	a	9.8
MW, ($\times 10^{-3}$)	596	182	54	19	9	a	a	171
alginate IV								
R_g , nm	61.3	33.6	26.1	14.7	8.7	5.6	3.3	32
wt fraction	0.166	0.366	0.258	0.128	0.055	0.019	0.010	
$[\eta]$, dL/g	25.29	14.74	8.73	5.02	3.6	a	a	12.7
MW, ($\times 10^{-3}$)	318	96	27	9	3	a	a	96
alginate VI								
R_g , nm	62.7	34.9	20.2	12.2	7.7	5.0	3.3	30
wt fraction	0.139	0.376	0.274	0.132	0.055	0.019	0.006	
$[\eta]$, dL/g	22.6	13.2	6.1	3.7	2.3	a	a	10.4
MW, ($\times 10^{-3}$)	380	121	42	15	5	a	a	112
alginate VII								
R_g , nm	53.9	30.4	18.1	11.3	7.4	4.9	3.3	25
wt fraction	0.123	0.363	0.277	0.145	0.062	0.025	0.008	
$[\eta]$, dL/g	17.0	8.5	3.8	2.0	1.3	a	a	6.6
MW, ($\times 10^{-3}$)	328	124	58	26	14	a	a	106
apple pectin								
R_g , nm	34.7	19.0	11.8	7.8	5.2	3.6	2.5	14
wt fraction	0.130	0.238	0.275	0.193	0.098	0.045	0.023	
$[\eta]$, dL/g	4.3	3.0	1.1	0.6	a	a	a	1.7
MW, ($\times 10^{-3}$)	365	81	42	24	a	a	a	83
gum arabic								
R_g , nm		22.5	14.3	10.4	7.6	5.4	3.7	12
wt fraction		0.061	0.301	0.488	0.109	0.034	0.008	

* Below detection limit.

i.v. of 7.2 ± 0.1 dL/g, and global R_{gw} of 43 nm were obtained (Table II). Just over 25% of the sample was high MW (component 1 $MW_w = 1\,147\,000$). The log(fitted i.v.) vs log(fitted R_{gw}) plot in Figure 7 is uniform and has a slope of 1.48 over a 10-fold change in R_{gw} . This result is consistent with an extended stiff chain conformation. Gralén and Kärholm (1950) reported for one purified fraction of tragacanthin, a complex acidic polysaccharide with a structure similar to that of pectin, a high molecular weight (840 000) and high viscosity. Extended stiff chains of this fraction had dimensions of 450 nm by 2 nm (Meer et al., 1973). Component 1 may possibly represent aggregated material. In the case for pectin, aggregates may result from chain-chain overlap interactions (junction zones) which maintain rigidity and an extended aggregate conformation (Fishman et al., 1993).

Gum Locust Bean. The HPSEC chromatogram was fitted by six concentration components and four viscosity components (Figure 8). The observed i.v. of 10.0 ± 0.1 dL/g at 35 °C was within the i.v. range 9.9–15.7 dL/g at 25 °C reported for a series of galactomannans (Dea et al., 1986). The global MW_w of 341 000 agrees with one literature value of 310 000 (Dea et al., 1986). A global R_{gw} of 43 nm and global i.v. of 10.2 dL/g were found (Table II). This polysaccharide had nearly 80% its weight fraction in components 1 and 2 (Table II). The log(fitted i.v.) vs log(fitted R_{gw}) plot was not uniform. This suggests at least the following possibilities: (1) This commercial preparation contains a mixture of galactomannans with different mannose/galactose ratios. (2) Aggregates may be present

and may have shapes significantly different from material represented by components 2–6 in Table II. The distribution of monoglucosyl side chains along the mannan backbone chain is clustered so that shorter galactomannan chains can be expected to exhibit some variation in physical properties. Chain-chain interactions are reported to occur between homomannan regions (Dea et al., 1986).

(Carboxymethyl)cellulose (CMC). The HPSEC chromatogram was fitted by seven concentration components and five viscosity components (Figure 9). An observed i.v. of 10.4 ± 0.1 dL/g was found and is within reported ranges for CMC at higher and lower ionic strength (Brown and Henley, 1964; Batdorf and Rossman, 1973). A global MW_w of 171 000, global i.v. of 9.8 dL/g, and global R_{gw} of 33 nm were obtained from component analysis. Fifty-eight percent of the CMC sample was represented by components 2 and 3, while 16% of the sample was high MW_w (590 000, component 1, Table II). Low MW_w component 4 and 5 material exhibited high viscosity characteristic of extended chains with high charge density. The log(fitted i.v.) vs log(fitted R_{gw}) plot in Figure 7 is slightly curved with a slope of 0.93 in the linear region between components 1 and 2. CMC component 1 is greater in i.v. and lesser in MW_w and R_{gw} than tragacanthin component 1. In contrast, the opposite relationships hold for alginate IV components. These relationships might possibly reflect either different aggregation behavior or differences in degree of chain extension and rigidity. In this investigation, CMC was well-behaved during sample preparation and HPSEC. Therefore, there is now an

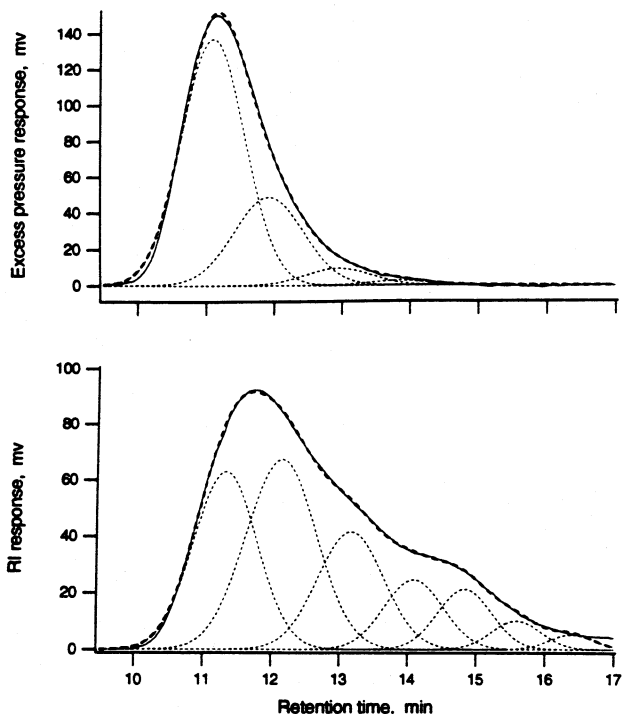


Figure 6. HPSE chromatogram of tragacanthin with concentration (RI) and viscosity (excess pressure) detection (solid line). Analysis gave seven concentration components with five matching viscosity components (light dashed lines). Heavy dashed line is the fitted total response of all the respective components.

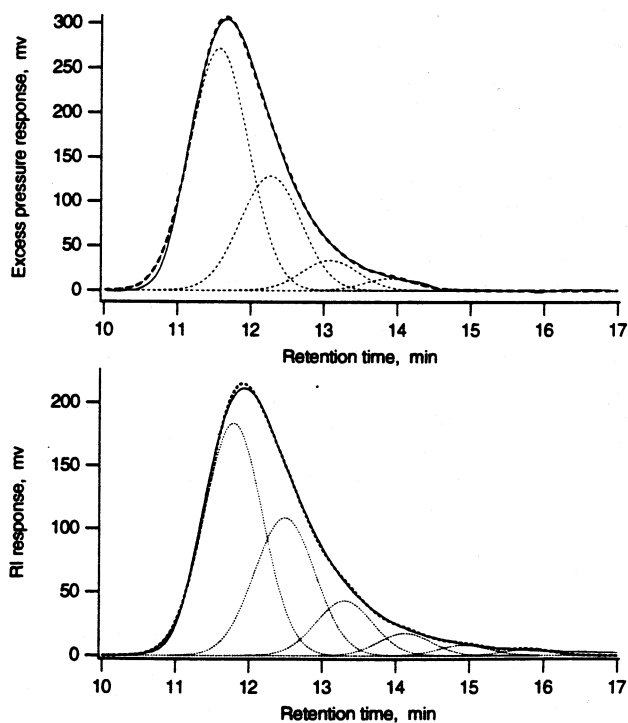


Figure 8. HPSE chromatogram of gum locust bean with concentration (RI) and viscosity (excess pressure) detection (solid line). Analysis gave six concentration components with four matching viscosity components (light dashed lines). Heavy dashed line is the fitted total response of all the respective components.

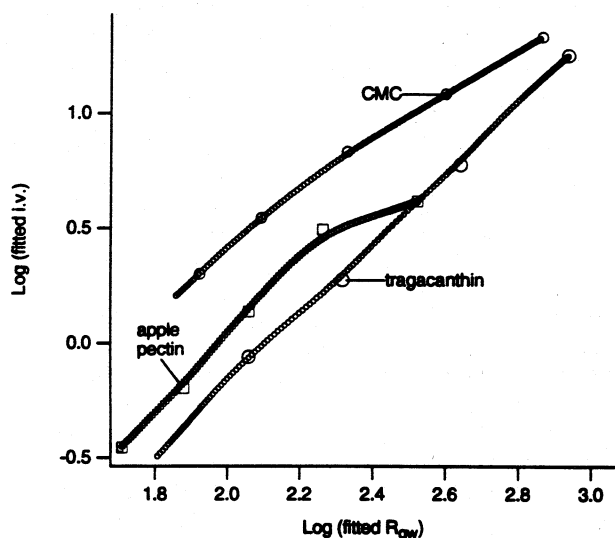


Figure 7. Power plots of $\log(\text{fitted i.v.})$ (eq 10) vs $\log(\text{fitted } R_{gw})$ (eq 11), small circles, and component $\log(\text{i.v.})$ vs component $\log(R_{gw})$ (Table II), large circles for tragacanthin, and CMC; squares for apple pectin.

opportunity to develop narrow R_{gw} distributed, purified, and stable fractions of CMC that could be used to calibrate HPSEC columns in terms of anionic polysaccharides.

Sodium Alginates. The HPSE chromatograms were fitted by seven concentration components and five viscosity components (Figure 10). The commercial alginates analyzed have i.v. values which decrease in the order IV > VI > VII (12.6 ± 0.2 , 10.5 ± 0.2 , 6.6 ± 0.1 dL/g). This ranking appears to be due to the decrease in both weight average of component 1 (0.17, 0.14, 0.12) and i.v. (25.3, 22.6, 17.0 dL/g) going from alginate IV to VII (Table II). With all three alginates, components 2 and 3 represent 62% of the eluted material. Freshly extracted sodium alginates from various algae have i.v. values from 12 to 16 dL/g, 0.2 M NaCl, 25 °C, and molecular weights from

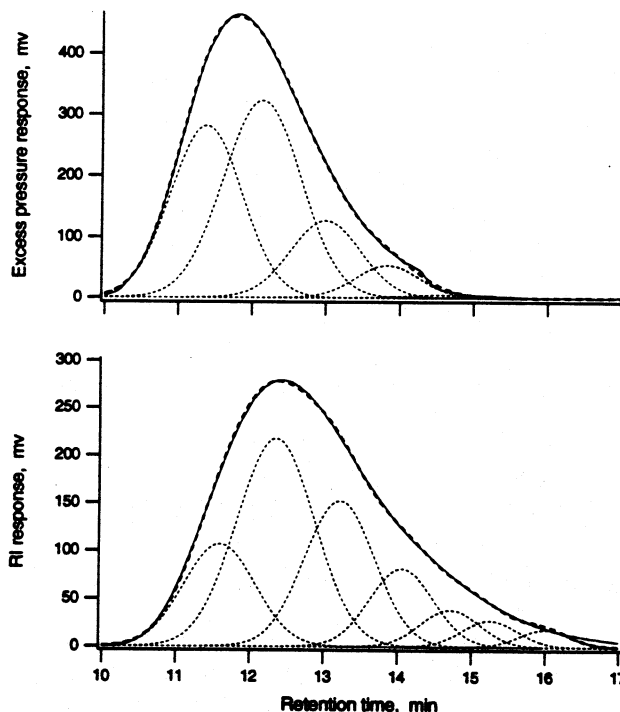


Figure 9. HPSE chromatogram of CMC with concentration (RI) and viscosity (excess pressure) detection (solid line). Analysis gave seven concentration components with five matching viscosity components (light dashed lines). Heavy dashed line is the fitted total response of all the respective components.

143 000 to 351 000 (Wedlock et al., 1987). Commercial alginates have molecular weights from 32 000 to 200 000 (Wedlock et al., 1987). Further processing, such as freeze-drying, reduces both i.v. and MW (Wedlock et al., 1987). After freeze-drying, the Mark-Houwink constant α in ($i.v. = kMW^\alpha$) drops from 0.76 to 0.59 (Wedlock et al., 1987). The Mark-Houwink constant of a series of well-charac-

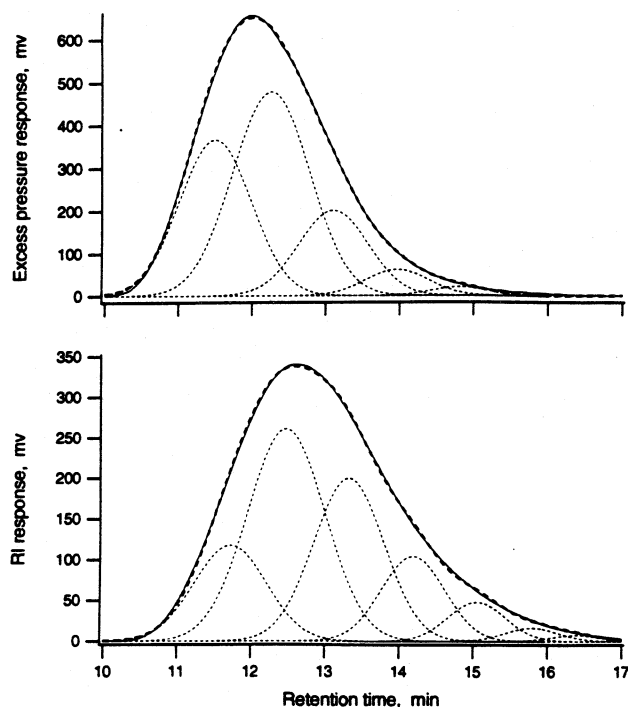


Figure 10. HPSEC chromatogram of sodium alginate IV with concentration (RI) and viscosity (excess pressure) detection (solid line). Analysis gave seven concentration components with five matching viscosity components (light dashed lines). Heavy dashed line is the fitted total response of all the respective components.

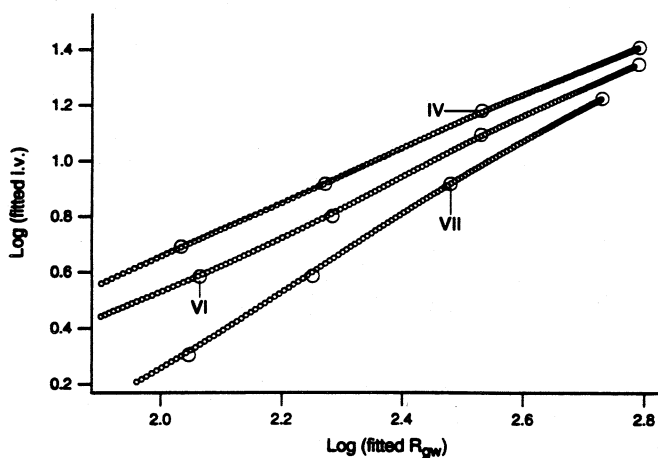


Figure 11. Power plots of $\log(\text{fitted i.v.})$ (eq 10) vs $\log(\text{fitted } R_{gw})$ (eq 11), small circles, and component $\log(\text{i.v.})$ vs component $\log(R_{gw})$, large circles, for alginates IV, VI, and VII (Table II).

terized alginates with polydispersity of 3 has been shown to be dependent on ionic strength (Smidsrød, 1970). Aggregation can influence the value of the Mark-Houwink constant as well as the apparent polydispersity. Component values for alginate weight fraction and MW_w in Table II give a polydispersity of 1.3–1.5. The $\log(\text{fitted i.v.})$ vs $\log(\text{fitted } R_{gw})$ plots in Figure 11 are linear over nearly a 10-fold R_{gw} span. Alginate IV has the highest i.v. and lowest slope of 0.94 compared to alginate VI (1.05) and alginate VII (1.17). Even though these commercial alginates may be neither highly purified nor compositionally homogeneous, component analysis gave a good power correlation between i.v. and R_{gw} , which suggests conformational uniformity throughout the distribution of sizes. The higher MW_w and lower i.v. values for alginate VII components may indicate some association of shorter chains with longer chains of component 1 and 2 material.

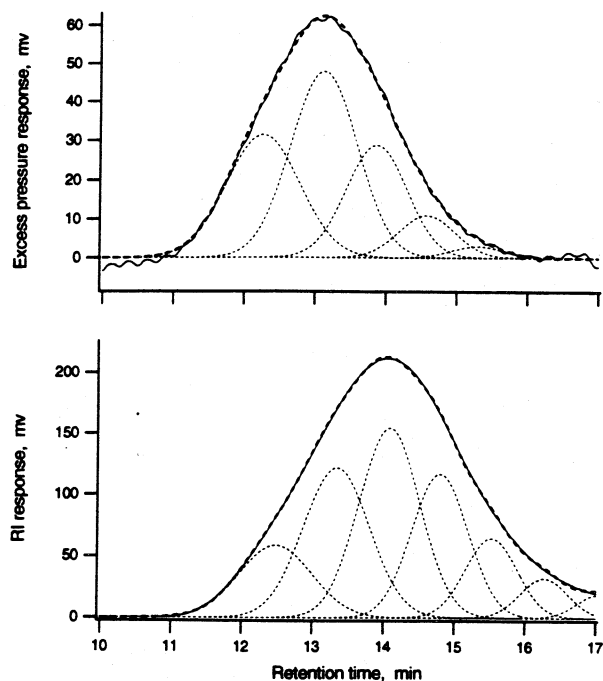


Figure 12. HPSEC chromatogram of apple pectin with concentration (RI) and viscosity (excess pressure) detection (solid line). Analysis gave six concentration components with four matching viscosity components (light dashed lines). Heavy dashed line is the fitted total response of all the respective components.

An alternative and not necessarily excluding explanation is that because of composition differences (i.e., guluronic/mannuronic ratios) alginate VII chains are more flexible and therefore exhibit less i.v. than chains of alginate IV and VI.

Apple Pectins. The HPSEC chromatogram was fitted by seven concentration components and four viscosity components (Figure 12). The observed i.v. of 1.8 ± 0.1 dL/g at 35 °C is within the range of i.v. values from 1.2 to 2.4 dL/g reported for apple pectins at 28–40 °C (Walter and Sherman, 1988; Sjöberg, 1987). A global MW_w of 83 000, global i.v. of 1.7 dL/g, and global R_{gw} of 14.0 nm were obtained from component analysis. The results with apple pectin quantitatively show that commercial apple pectin has component R_g values similar to those for grapefruit, pea skin, garlic skin, and garlic foliage pectins (Fishman et al., 1991a). The low observed i.v. for this commercial apple pectin sample can be attributed to component 2, 3, and 4 material which comprised 81% of the sample weight (Table II). The $\log(\text{fitted i.v.})$ vs $\log(\text{fitted } R_{gw})$ plots in Figure 7 show distinct downward curvature going from component 2 to 1. On the basis of a similar observation with lime pectin (Hoagland et al., 1993) and the recent report of pectin microgel particles (Fishman et al., 1992), this curvature could result from association of low MW apple pectin into more compact, aggregates with i.v. lower than expected for single long, extended chains of comparable MW.

Gum Arabic. The HPSEC chromatogram was fitted by six concentration components (Figure 13). As can be seen in Figure 13, the excess pressure response was too low for accurate determination of viscosity components. An observed i.v. of 0.145 ± 0.003 dL/g, and global R_{gw} of 11.8 ± 0.1 nm were obtained. Values of 500 000 for MW (Blake et al., 1988) and 0.20 dL/g for i.v. have been reported (Anderson and Rahman, 1967). The HPSEC results for gum arabic were consistent with a high molecular weight polysaccharide with a compact, flexible shape, such as a sphere or a tight stiff spiral with many side chains, that

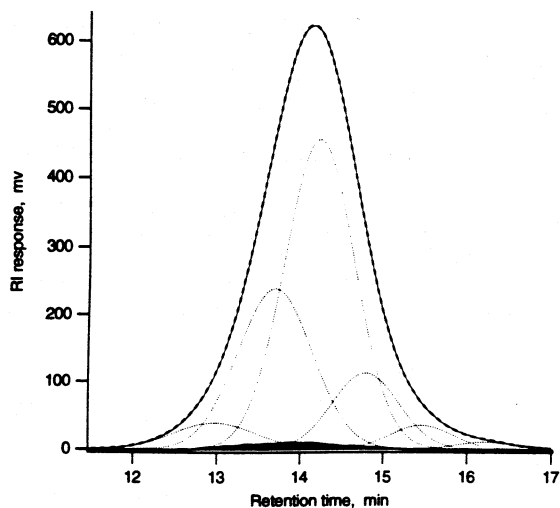


Figure 13. HPSEC chromatogram of gum arabic with concentration (RI) and viscosity (excess pressure) detection (solid fill). Analysis gave six concentration components (light dashed lines). Heavy dashed line is the fitted total response of all the concentration components.

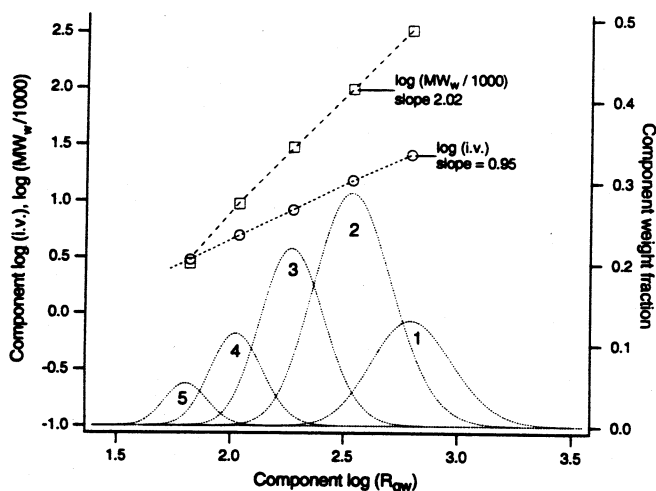


Figure 14. Power plots of component $\log(i.v.)$, circles, and component $\log(MW_w)$, squares, vs component $\log(R_{gw})$ (Table II) and distribution of component weight as a function of $\log(R_{gw})$ for alginate IV. Dashed lines are linear fits with indicated slopes.

exhibits low viscosity (Qi et al., 1991). Commercial preparations of gum arabic are possibly mixtures of an undegraded, highly glycosylated peptide and linear polysaccharides detached from the native peptide (Randall et al., 1988; Qi et al., 1991).

Power Relationships. For a polysaccharide that has a characteristic conformation for a range of molecular sizes or aggregate sizes, component analysis can provide power law exponents from plots of $\log(\text{fitted } i.v.)$ vs $\log(\text{fitted } R_{gw})$ and component $\log(MW_w)$ vs component $\log(R_{gw})$ as is shown in Figure 14 for alginate IV. The observed distribution of sizes from HPSEC is a result of dynamic interactions between solute polysaccharide molecules or aggregates, mobile phase ionic strength and pH, and column packing material. If adsorption effects are negligible, fractionation is a function of hydrodynamic volume and thereby related to R_{gw} by calibration. The distribution of sizes obtained by HPSEC is assumed to be directly correlated to distribution of sizes of the polysaccharide dissolved in mobile phase. Component analysis has the potential of uniquely characterizing a given polysaccharide in terms of both component weight fractions and power law exponents.

CONCLUSIONS

HPSEC with concentration and viscosity detection offers the following information after component analysis:

- global $i.v.$
- global R_{gw} , R_{gz}
- global MW_w , MW_z
- evidence for aggregation
- aggregate properties (MW_w , $i.v.$, R_{gw})
- exponents relating component MW_w , $i.v.$ and R_{gw}
- characteristic component weight fractions

This information can be useful for detection of adulteration, for quality control, for monitoring polymer processing, and for fundamental solution behavior of aggregating water-soluble polysaccharides. Costs for determination of R_g , $i.v.$, and MW of polysaccharides by HPSEC in terms of time and instrumentation can be greatly reduced when compared to those by light scattering, sedimentation, and traditional viscometers that require serial dilutions. HPSEC is performed with small volumes of dilute solutions that can be preconditioned with guard columns. HPSEC systems are currently being strengthened by the development of light scattering detectors, which will provide independent determination of MW_w and R_{gz} of large component size material.

LITERATURE CITED

- Anderson, D. M. W.; Rahman, S. Studies on uronic acid materials. Part XX. The viscosity-molecular weight relationship for *Acacia* gums. *Carbohydr. Res.* 1967, 4, 298-304.
- Batdorf, J. B.; Rossman, J. M. In *Industrial Gums*, 2nd ed.; Whistler, R., Ed.; Academic Press: New York, 1973; 704 pp.
- Blake, S. M.; Deeble, D. J.; Phillips, G. O.; Du Plessey, A. The effect of sterilizing doses of γ -irradiation on the molecular weight and emulsification properties of gum arabic. *Food Hydrocolloids* 1988, 2, 407-415.
- Brown, W.; Henley, D. Cellulose derivatives. IV. The configuration of the polyelectrolyte sodium carboxymethyl cellulose in aqueous sodium chloride solutions. *Makromol. Chem.* 1964, 79, 68-88.
- Dea, I. C. M.; Clark, A. H.; McCleary, B. V. Effect of the molecular fine structure of galactomannans on their interaction properties—the role of unsubstituted sides. *Food Hydrocolloids* 1986, 1, 129-140.
- Fishman, M. L.; Damert, W. C.; Phillips, J. G.; Barford, R. A. Evaluation of root-mean-square radius of gyration as a parameter for universal calibration of polysaccharides. *Carbohydr. Res.* 1987, 160, 215-225.
- Fishman, M. L.; Gillespie, D. T.; Sondey, S. M.; Barford, R. A. Characterization of pectins by size exclusion chromatography in conjunction with viscosity detection. *J. Agric. Food Chem.* 1989a, 37, 584-591.
- Fishman, M. L.; Gross, K. C.; Gillespie, D. T.; Sondey, S. M. Macromolecular components of tomato fruit pectin. *Arch. Biochem. Biophys.* 1989b, 274, 179-191.
- Fishman, M. L.; El-Atawy, Y. S.; Sondey, S. M.; Gillespie, D. T.; Hicks, K. B. Component and global average radii of gyration of pectins from various sources. *Carbohydr. Polym.* 1991a, 15, 89-104.
- Fishman, M. L.; Gillespie, D. T.; Sondey, S. M.; El-Atawy, Y. S. Intrinsic viscosity and molecular weight of pectin components. *Carbohydr. Res.* 1991b, 215, 91-104.
- Fishman, M. L.; Cooke, P.; Levaj, B.; Gillespie, D. T.; Sondey, S. M.; Scorza, R. Pectin microgels and their subunit structure. *Arch. Biochem. Biophys.* 1992, 294, 253-260.
- Fishman, M. L.; Gillespie, D. T.; Levaj, B. Structural analysis of aggregated polysaccharides by HPSEC/viscometry. In *Chromatography of Polymers: Characterization By SEC and FFF*; Provder, T., Ed.; ACS Symposium Series 521; American Chemical Society: Washington DC, 1993; pp 314-325.
- Flory, P. J. In *Principles of Polymer Chemistry*; Cornell University Press: Ithaca, NY, 1953; 611 pp.

- Gralén, N.; Kärrholm, M. The physicochemical properties of solutions of gum tragacanth. *J. Colloid Sci.* 1950, 5, 21-36.
- Hoagland, P. D.; Konja, G.; Fishman, M. L. Disaggregation of pectin during plate module ultrafiltration. *J. Food Sci.* 1993, 58, 680-687.
- Kato, T.; Okamoto, T.; Tokuya, T.; Takahashi, A. Solution properties and chain flexibility of pullulan in aqueous solution. *Biopolymers* 1982, 21, 1623-1633.
- Meer, G.; Meer, W. A.; Gerard, T. In *Industrial Gums*, 2nd ed.; Whistler, R., Ed.; Academic Press: New York, 1973; pp 291-293.
- Press, W. H.; Flannery, B. P.; Teukolsky, S. A.; Vetterling, W. T. In *Numerical Recipes in C*; Cambridge University Press: NY, 1988; 547 pp.
- Qi, W.; Fong, C.; Lamport, D. T. A. Gum arabic glycoprotein is a twisted hairy rope. *Plant Physiol.* 1991, 96, 848-855.
- Randall, R. C.; Phillips, G. O.; Williams, P. A. The role of the proteinaceous component on the emulsifying properties of gum arabic. *Food Hydrocolloids* 1988, 2, 131-140.
- Sjöberg, A.-M. The effects of γ -irradiation on the structure of apple pectin. *Food Hydrocolloids* 1987, 1, 271-276.
- Smidsrød, O. Solution properties of alginate. *Carbohydr. Res.* 1970, 13, 359-372.
- Walter, R. H.; Sherman, R. M. Application of intrinsic viscosity and the interaction coefficient to some ionic galacturonan dispersions. *Food Hydrocolloids* 1988, 2, 151-158.
- Wedlock, D. J.; Fasihuddin, B. A.; Phillips, G. O. Factors influencing the molecular weight of sodium alginate preparations. *Food Hydrocolloids* 1987, 1, 207-213.

Received for review December 7, 1992. Accepted May 11, 1993.